1 The ALEPH Experiment at the LEP e^+e^- Collider [1]

(1997–2003: W. Blum, V. Büscher, H. Carstens, G. Cowan, A. David, H. Dietl, H. Fischer, G. Ganis, U. Grenzemann, K. Hartkorn, A. Heister, K. Hüttmann, G. Lütjens, W. Männer, C. Mannert, H.-G. Moser, A. Rosado, S. Schael, R. Settles, M. Stehle, H. Seywerd, H. Stenzel, M. Villegas, G. Waltermann, W. Wiedenmann, G. Wolf)

1.1 The LEP Era

The four experiments at the Large Electron-Positron (LEP) storage ring in CERN have been dismantled after completing 12 years of data-taking, encompassing e^+e^- centre-of-mass energies ($\sqrt{s}$) from 88 to 209 GeV. It was an enormously successful period with an outpouring of over a thousand physics publications from the four experiments which have 'changed the face of particle physics'.

Our MPI für Physik had the pleasure of being a major player among the 32 institutes forming the ALEPH collaboration, from design through to hardware and physics realisation, and of experiencing a total of two decades of excitement in which the Standard Model (SM) was tested with unprecedented precision. The next couple of pages are obviously so few that only give a hint of the happenings can be conveyed.

ALEPH Detector

ALEPH, A detector for LEP PHysics, measured the particles emanating from the e^+e^- annhiliation over 98% of the full solid angle surrounding the interaction point, as seen in Fig. 1. The concept of a precise vertex detector, a large central tracker and an electromagnetic calorimeter, all highly granular and all inside a 1.5T magnetic solenoid, proved to be a very powerful combination for the physics analyses.

The MPI-ALEPH group was responsible (concept, design, construction, maintainence) for major parts of the tracking and data acquision:

• The vertex detector (VDET) consisted of two concentric cylinders of double-sided silicon-strip detectors mounted to within 60 mm of the beamline. The high precision ($\sigma_{point} = 12\ \mu$m) and closeness to the interaction point enables the reconstruction of heavy 'long'-lived (O(mm)) particles, e.g., B-hadrons, τ-leptons. Items designed and built by MPI-Munich included the microelectronic readout, detectors and support mechanics.

• The Time Projection Chamber (TPC) measured 3D space points and ionisation of charged particles to yield momenta and mass identification for these tracks. The momentum accuracy by the ALEPH TPC and VDET combined was unsurpassed among the world's collider detectors. MPI-Munich designed and constructed the TPC wire-chamber sectors and frontend electronics.

• The third-level trigger was a computing farm which filters away background events by a fast (msec) online analysis of the subdetector information. Our institute designed and programmed this device.

All above components from MPI-Munich functioned well during the 12-year period with only maintainence (no major disasters) occurring.

LEP Machine

The first phase of data acquisition (called LEP1) in the years 1989–1995 covered the Z resonance with 200 pb^{-1} per experiment taken over a range of energies $\sqrt{s} \sim$ 88–95 GeV, and the parameters of the SM were measured to an accuracy which surpassed original expectations by an order of magnitude.

The machine energy was then systematically increased during the second phase (LEP2) over the years 1995–2000: $\sqrt{s} \sim$ 130–136, 161–172, 183, 189, 192–202 GeV, culminating in year 2000 with the energy pushed to the limit $\sqrt{s} \sim$ 204–209 GeV in search of the SM Higgs boson. And tantalizing evidence was seen for it, as described below. Other main LEP2 goals included the precise measurement of the W-boson and search for Supersymmetry.

Altogether (LEP1 + LEP2) better than 1 fb^{-1} of data per experiment was accumulated.

1.2 Physics 1997-2003

The e^+e^- data from LEP touches almost all of particle physics. And the MPI-ALEPH group was involved in practically all aspects of LEP physics – Electroweak, τ, Heavy Flavour, QCD, Supersymmetry and Higgs – in addition to hardware, data-taking and analysis responsibilities. A picture book of examples follows.

• Detector hardware – Fig. 1.

The general performance is characterized by
·track momentum: $\delta(\frac{1}{p_t}) \leq 6 \cdot 10^{-4} (\mathrm{GeV/c})^{-1}$,
·flavour tagging: $\delta(IP_{r\phi,z}) \leq 25\mu\mathrm{m} + \frac{95\mu\mathrm{mGeV/c}}{p \sin^{3/2}\theta}$

[1] Supported in part by the federal ministry BMBF

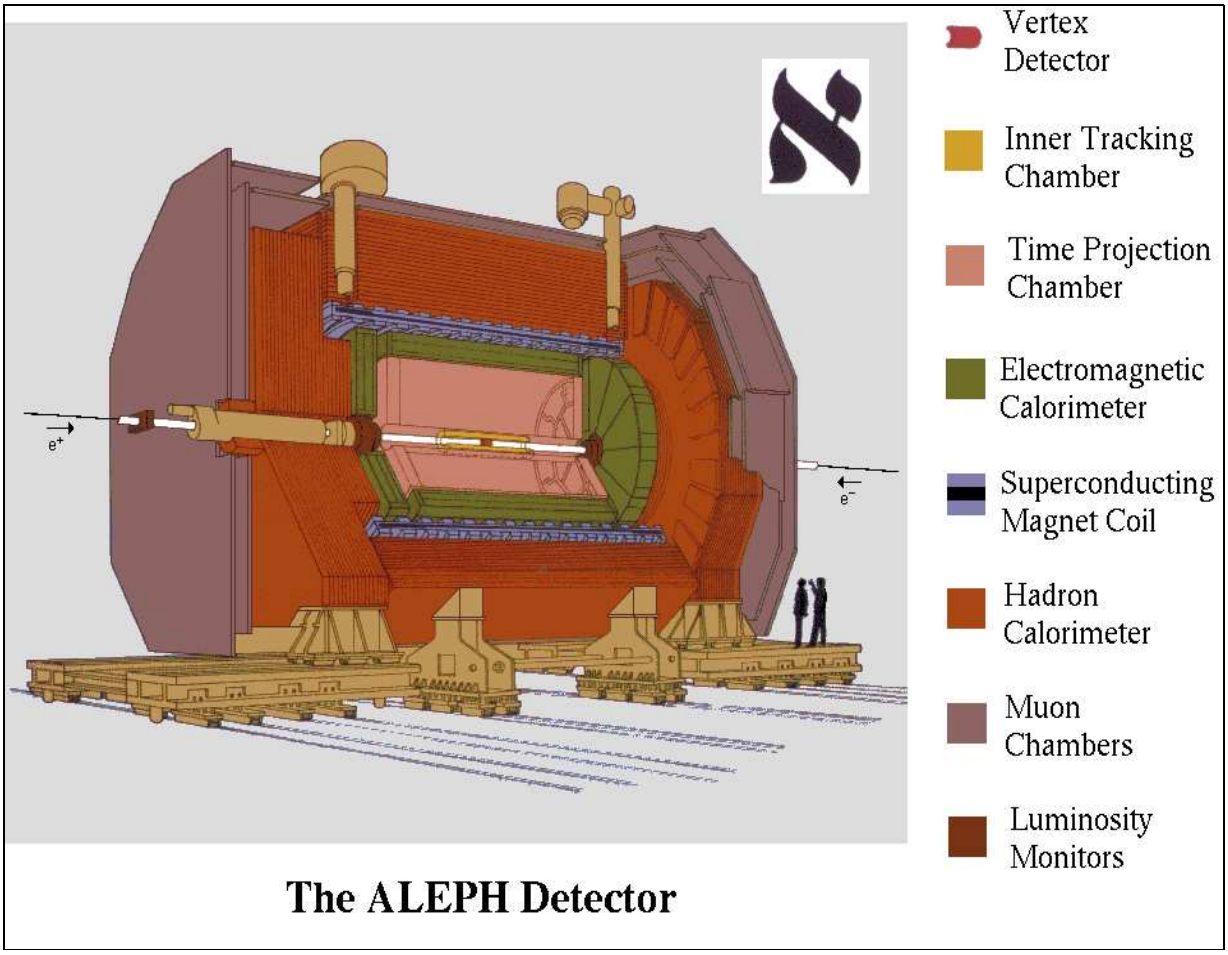

Figure 1: The hardware.

·energy flow: $\frac{\delta E}{E} \simeq 0.6 \frac{1}{\sqrt{E}}$ (E in GeV) and
·hermeticity: forward coverage down to 24 mrad.

• Tests of electroweak theory – Fig. 2.

The precision at LEP1 turned out 10 × better than first planned and confirmed higher-order radiative calculations of the SM to the 10^{-4} level (for ALEPH alone and much better for the LEP combined data). Radiative emission of virtual top quarks for example enabled the indirect measurement $M_{top} = 192\pm\ 12$ GeV/c^2, later confirmed by direct production at the Tevatron. Subsequently indirect evidence for the Higgs is being pursued (see below).

The cross sections Fig. 2(a) yield the determination of the total Z width (Γ_Z) and of the partial decay widths into hadrons (Γ_{had}) and leptons (Γ_{lep}). The ALEPH measurements infer the number of light neutrinos to be $N_\nu = 2.983 \pm 0.013$, and lepton universality of the Z couplings is tested to the 0.2% level.

The forward-backward asymmetries are sensitive to the weak mixing angle $\sin^2\theta_W$. A fruitful collaboration with our MPI theory group pioneered the forward-backward asymmetry measurement using the so-called 'hemisphere charge method'. The latest compilation of these asymmetries is seen in Fig. 2(b), where they are interpreted in terms the 'effective' weak mixing angle which also depends on the Higgs boson mass.

The cross section plus forward-backward asymmetry precision allows disentangling the initial and final state Z couplings to leptons in a fit for individual the effective vector and axial couplings g_{Ve}, $g_{V\mu}$, $g_{V\tau}$, g_{Ae}, $g_{A\mu}$ and $g_{A\tau}$, as exemplified the Fig. 2(c). The shaded area indicates the SM expectation for $M_{top} = 174\pm5$ GeV/c^2 and $90 < M_H < 1000$ GeV/c^2; the vertical fat arrow shows the change if the electromagnetic coupling constant is varied within $1/\alpha(M_Z) = 128.886\pm0.090$.

It can be noticed from Figs. 2 (b) and (c) that a light Higgs mass is favoured by the data.

• Properties of heavy quarks – Fig. 3.

An intriging result comes from the fact that B^0_s mesons are predicted to oscillate between particle and antiparticle types during their lifetime due to box diagrams

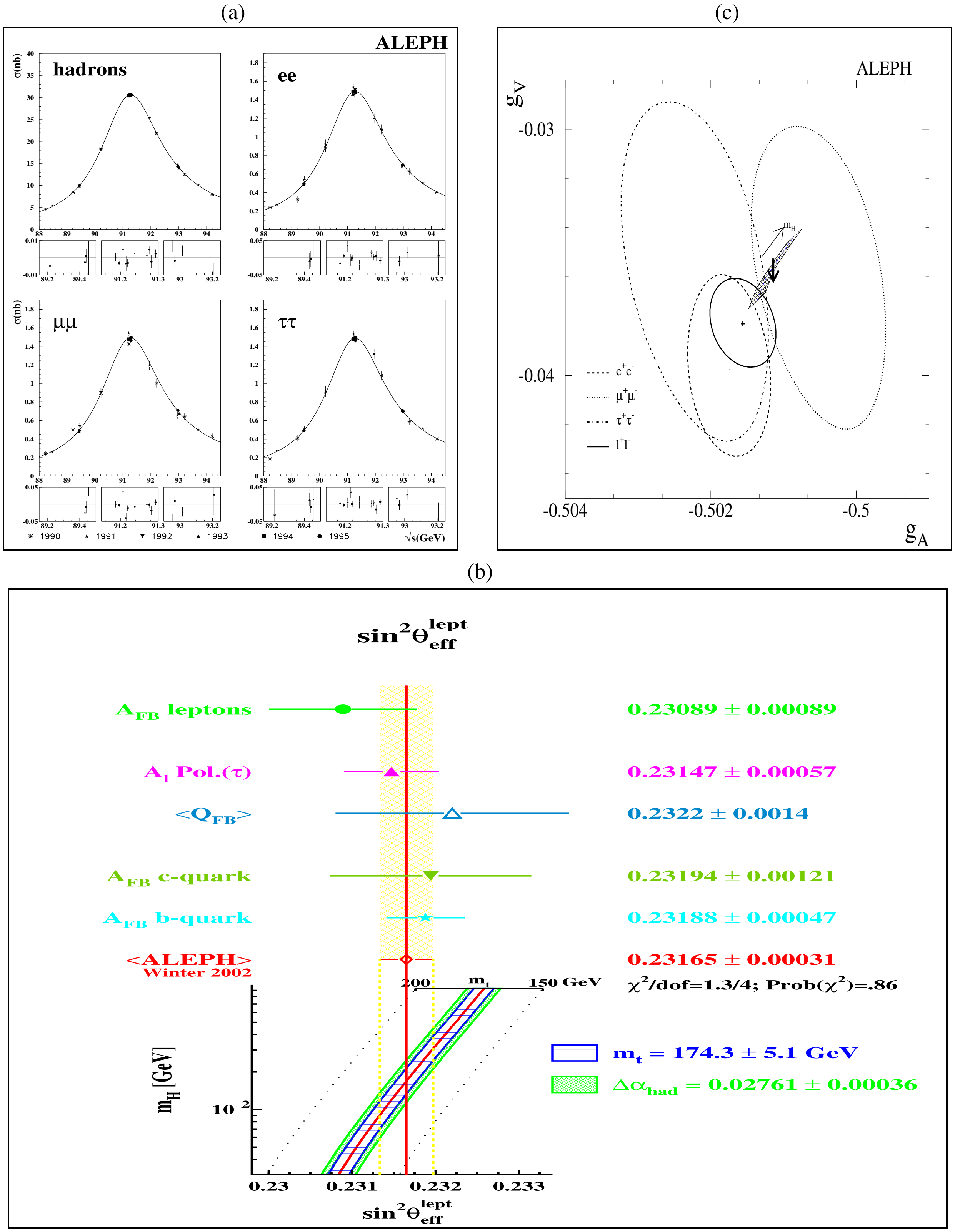

Figure 2: (a) Z resonance measurements and comparison with SM predictions for 3 light neutrino generations. (b) Forward-backward asymmetry measurements. (c) The one-σ contours of the effective lepton couplings. (See text.)

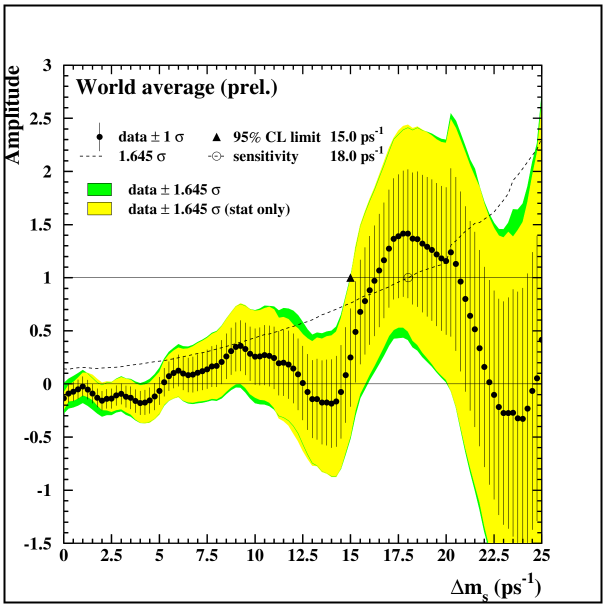

Figure 3: Status for B_s^0 oscillations. (See text.)

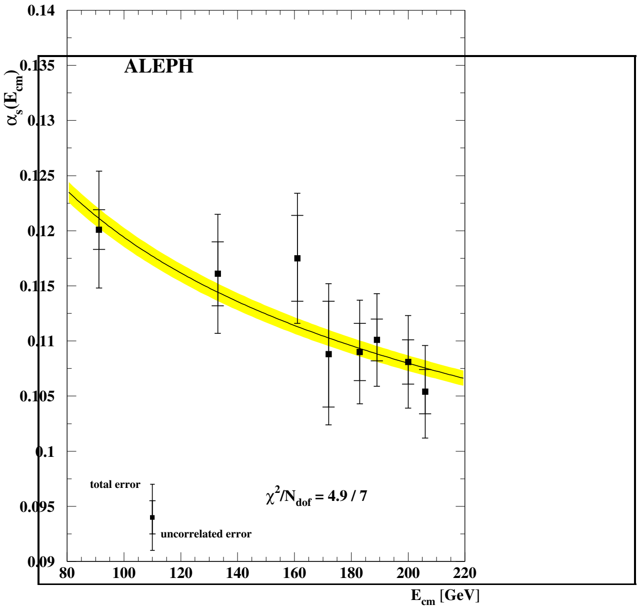

Figure 4: ALEPH's final result for α_s measured at LEP1 and LEP2. The curve is fit to the data using the three-loop running formula and corresponds $\Lambda_{\bar{MS}} = 247 \pm 14$ MeV, which is equivalent to $\alpha_s(M_Z) = 0.1211 \pm 0.0008$. (See text.)

connecting the two states. Many techniques are used to tag the (anti)particle type at production and decay, and the so-called 'amplitude method' developed by our group for combining different analyses is now used universally to obtain the maximum sensitivity. The world situation for B_s^0 oscillations is shown in Fig. 3. The points with error bars are the average of the osciallation amplitudes measured by the world labs. The data at high oscillation frequency is dominated by the ALEPH and SLD experiments. The yellow (grey) region gives the 95 % confidence interval, the dotted line is the expected sensitivity, and where they cross unity amplitude marks the experimental limit, 15 ps^{-1}. Debates are raging as to whether the bump at $\sim$ 18 ps^{-1} indicates a true signal or not.

• QCD studies – Figs. 4 and 5.

Many measured distribution and model fits as a function of $\sqrt{s}$ could be shown, such as charged multiplicity, particle momenta and angles, event shapes, jet rates and the strong coupling constant α_s. We choose here to show in Fig. **??** the final result for α_s which was recently published, namely

$$\alpha_s(M_Z) = 0.1214 \pm 0.0048$$

where the error is dominated by theoretical uncertainties (the statistical uncertainty is indicated in the figure caption).

The well-known Bose-Einstein enhancement of phase space for identical bosons becomes a de-enhancement for identical fermions, as clearly seen for events in which a pair of Λs were produced. Figure 5(upper) depicts the correlation $C(Q)$ as function of the four-momentum transfer Q between the two Λs in the same event, where $C(Q)$ is differential cross section $d\sigma/dQ$ for ΛΛ–pairs normalised to that of three different reference samples: A) Monte Carlo events, B) experimental data using hyperons from different events and C) experimental data, but with the hyperons from different events weighted so as to reproduce the experimental angular distribution. The curves are the 'Goldhaber' function for a Gaussian source, $1 - be^{-(RQ)^2}$. The fitted parameters are $b = 0.6 \pm 0.1$ und $R = 0.11 \pm 0.02$ fm.

Further measurements have been performed using pp,$\bar{p}\bar{p}$ pairs and $K_s^0 K_s^0$ pairs. These are also shown in Fig. 5 using analogous reference samples A) and B). The former again show a suppression which could be attributed to Fermi-Dirac statistics, while the latter shows the Bose-Einstein enhancement. The fitted parameters are $b = 0.5 \pm 0.1$ und $R = 0.10 \pm 0.02$ fm for the former and and $b = 0.6 \pm 0.2$ und $R = 0.6 \pm 0.12$ fm for the latter.

These results for the source radius and those from other experiments are plotted as a function of particle mass in the lower figure, where it can be seen that the radius decreases for increasing mass. Debates are raging as to the reason for this effect.

• Search for Supersymmetry – Fig. 6.

Supersymmetry (Susy) is such an attractive extension

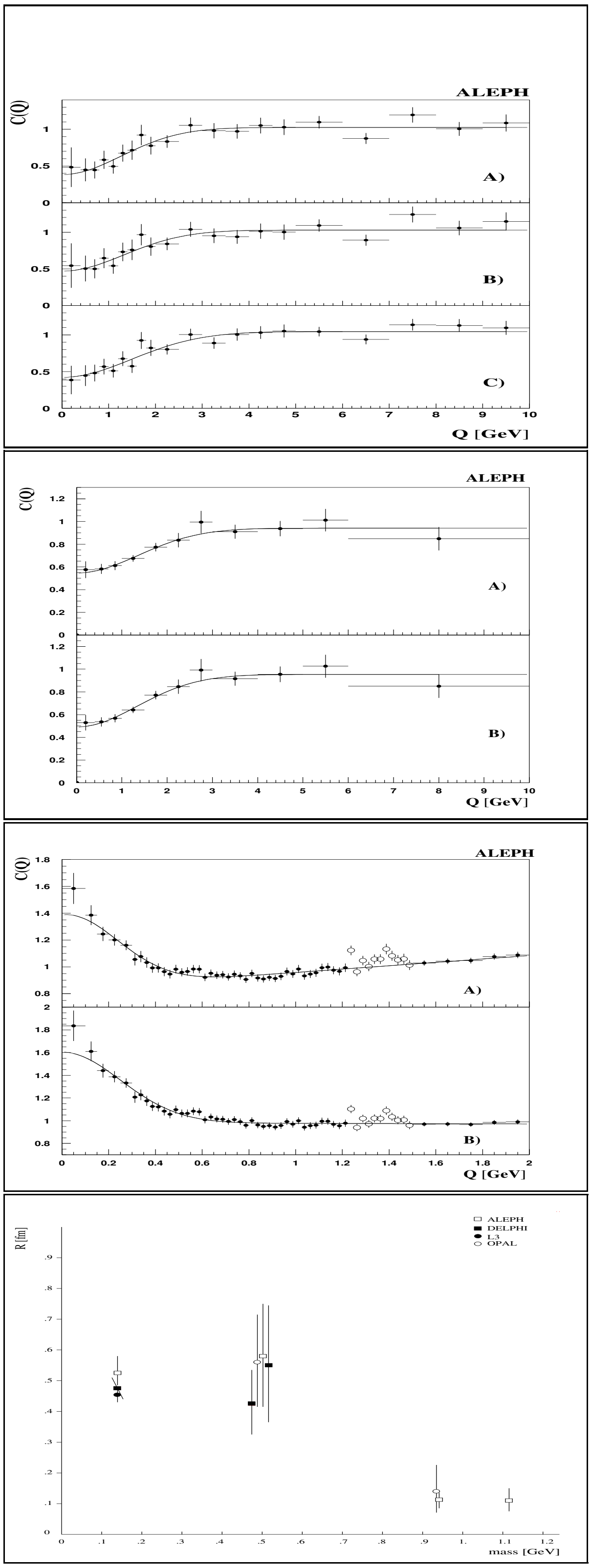

Figure 5: Upper: Correlation $C(Q)$ for $\Lambda\Lambda$ pairs for three reference samples. Middle: Correlation $C(Q)$ for pp, $\bar{p}\bar{p}$ pairs for two reference samples. Middle: Correlation $C(Q)$ for $K^0_s K^0_s$ pairs for two reference samples. Lower: Overview of results for R plotted as a function of particle mass. (See text.)

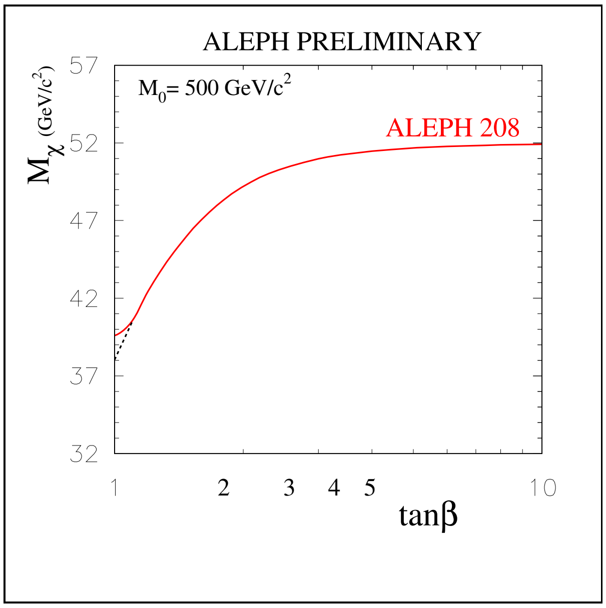

Figure 6: Limit for the mass of the LSP in gravity-mediated Susy breaking (the region under the curve is excluded). (See text.)

of the SM that it would be a pity if it did not exist. This model has several nice features: it predicts the correct value for $\sin^2\theta_W$, explains the generation the higgs mechanism for large M_{top}, is a solution for the heirarchy problem, gauge-coupling unification, dark matter, for example. Interestingly enough, it predicts the Higgs to be light ($m_H < 130$ GeV/c^2).

Susy postulates a symmetry between fermions and bosons. For every SM fermion there is supersymmetic spin-0 partner (sfermion: sbottom, stau) of the same mass, and similarly the SM bosons have Susy spin-$\frac{1}{2}$ partners (the '...inos': gaugeinos, Higgsinos, etc.). This symmetry is obviously broken since the spartners do not exist at the same mass, and there are several Susy-breaking mechanisms on the market. While it is outside the scope of this article to even try to list all of the parameters of the Susy models, a couple of examples will be seen below.

At LEP a tremendous intellectual and physical effort was invested in Susy searches. Unfortunately no direct evidence was found, but the Susy parameter space has been sensitively narrowed. Two (out of a hundred possibile) example are shown here.

For the first, the Susy breaking is assumed to stem from a coupling to gravity. Lepton, baryon and Susy (so-called 'R-parity') quantum numbers are conserved. Then the lightest Susy particle (LSP) is stable and is often taken to be the neutralino χ, a spartner of the Z, γ and Higgs bosons, and is also the source of

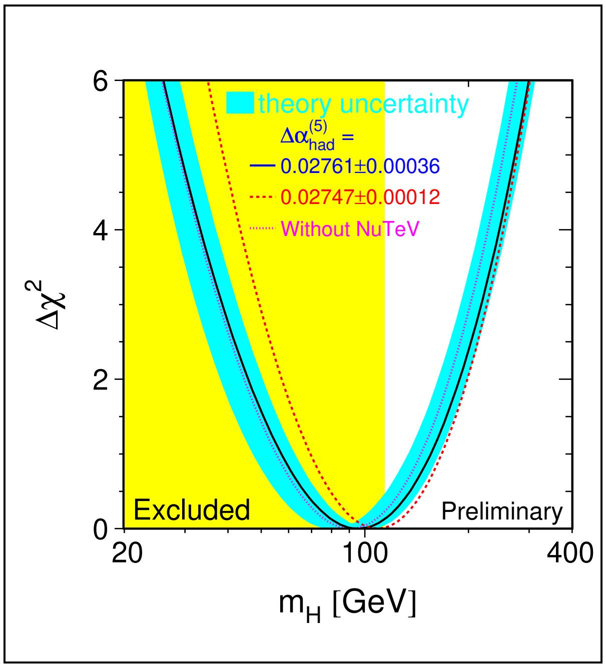

Figure 7: Fit of the SM with m_{Higgs} as free parameter to the world electroweak data. (See text.)

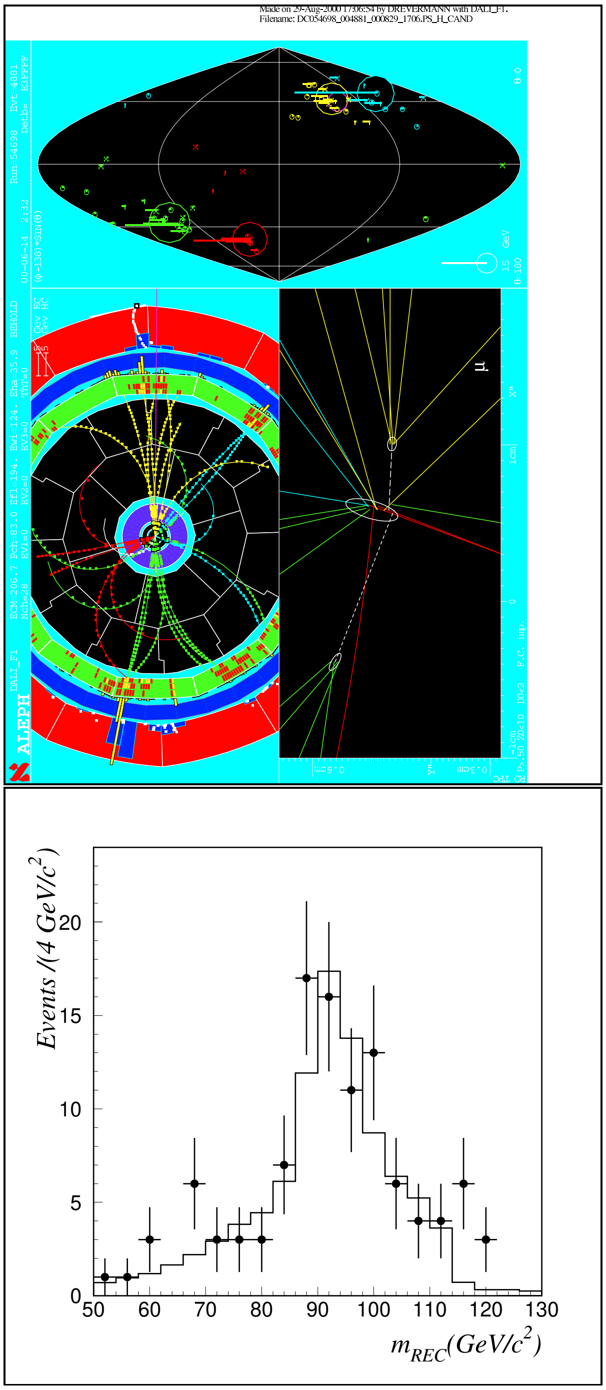

Figure 8: Excess seen in the neutral SM Higgs search. Upper: a candidate with mass = 114 GeV/c^2. Lower: mass plot of all candidates.

cold dark matter. Figure 6 shows the limit on the χ mass as a function of $\tan\beta$, the ratio of the vacuum expectation values for the two higgs fields in Susy, and for one value of M_0, the gauge unification mass.

• Search for Higgs boson – Figs. 7 and 8.

The MPI-Aleph group has been involved in searches for both charged and neutral Higgs bosons. The status of the now-famous blueband plot of the combined electroweak data with the SM Higgs as parameter is shown in Fig. 7(upper), which confirms evidence seen earlier (Fig. 2) that the Higgs is indicated to be light.

The search for the standard SM Higgs was more successful and produced an fascinating fluctuation. In the closing months of operation LEP was running in the 'Higgs discovery mode'. During each 'fill' of the machine with beam the energy was pushed to the limit of the acceleration capability of the superconducting cavaties: $\sqrt{s} \sim$ first 205, then 207 and finally 209 GeV, until a quench of a superconducting cavity cause the beam to be lost. The fills would last up to an hour, and after beam loss the machine was refilled and the procedure repeated.

LEP managed to accumulate about 150 pb^{-1} above 206 GeV, and the results for the Higgs search in ALEPH are shown in Fig. 8. Three of the candidates found were 'golden', one of which is seen on the cover of this report and another one in Fig. 8. Most of the candidates were consistent with SM background, except to the 'bump' of events around 115 GeV. This bump contains the three 'golden' canditates mentioned above and is about 3σ above the expected background.

The LEP machine and experiments were stopped at the end of year 2000, so judgement on this 3σ effect will have to wait for the Tevatron and the LHC.